Clin Pharmacokinet
DOI 10.1007/s40262-016-0447-7

ORIGINAL RESEARCH ARTICLE

# Physiologically Based Pharmacokinetic Modeling to Predict Drug–Drug Interactions with Efavirenz Involving Simultaneous Inducing and Inhibitory Effects on Cytochromes

**Catia Marzolini[1,2] · Rajith Rajoli[3] · Manuel Battegay[1,2] · Luigia Elzi[4] · David Back[3] · Marco Siccardi[3]**



**Abstract**

*Background* Antiretroviral drugs are among the therapeutic agents with the highest potential for drug–drug interactions (DDIs). In the absence of clinical data, DDIs are mainly predicted based on preclinical data and knowledge of the disposition of individual drugs. Predictions can be challenging, especially when antiretroviral drugs induce and inhibit multiple cytochrome P450 (CYP) isoenzymes simultaneously.

*Methods* This study predicted the magnitude of the DDI between efavirenz, an inducer of CYP3A4 and inhibitor of CYP2C8, and dual CYP3A4/CYP2C8 substrates (repaglinide, montelukast, pioglitazone, paclitaxel) using a physiologically based pharmacokinetic (PBPK) modeling approach integrating concurrent effects on CYPs. In vitro data describing the physicochemical properties, absorption, distribution, metabolism, and elimination of efavirenz and CYP3A4/CYP2C8 substrates as well as the CYP-inducing and -inhibitory potential of efavirenz were obtained from published literature. The data were integrated in a PBPK model developed using mathematical descriptions of molecular, physiological, and anatomical processes defining pharmacokinetics. Plasma drug–concentration profiles were simulated at steady state in virtual individuals for each drug given alone or in combination with efavirenz. The simulated pharmacokinetic parameters of drugs given alone were compared against existing clinical data. The effect of efavirenz on CYP was compared with published DDI data.

*Results* The predictions indicate that the overall effect of efavirenz on dual CYP3A4/CYP2C8 substrates is induction of metabolism. The magnitude of induction tends to be less pronounced for dual CYP3A4/CYP2C8 substrates with predominant CYP2C8 metabolism.

*Conclusion* PBPK modeling constitutes a useful mechanistic approach for the quantitative prediction of DDI involving simultaneous inducing or inhibitory effects on multiple CYPs as often encountered with antiretroviral drugs.

✉ Catia Marzolini
catia.marzolini@usb.ch

[1] Division of Infectious Diseases and Hospital Epidemiology, Department of Medicine, University Hospital of Basel, Petersgraben 4, 4031 Basel, Switzerland

[2] Division of Infectious Diseases and Hospital Epidemiology, Department of Clinical Research, University Hospital of Basel, Petersgraben 4, 4031 Basel, Switzerland

[3] Department of Molecular and Clinical Pharmacology, Institute of Translational Medicine, University of Liverpool, Liverpool, UK

[4] Division of Infectious Diseases, Regional Hospital Bellinzona, Bellinzona, Switzerland

Published online: 07 September 2016

**Key Points**

The developed physiologically based pharmacokinetic model integrating mixed effects on cytochrome P450 (CYP) isoenzymes represents a useful tool for the quantitative prediction of drug–drug interactions (DDIs) involving inhibitory and inducing effects on multiple CYPs as often encountered with HIV drugs.

The overall effect of efavirenz on dual CYP3A4/CYP2C8 substrates is induction of metabolism. The magnitude of induction tends to be less pronounced for dual CYP3A4/CYP2C8 substrates with predominant CYP2C8 metabolism.

Dosage adjustments can be simulated to overcome a given interaction. Thus, this model has the potential to provide guidance on how to manage DDIs for drug combinations used in clinical practice for which no clinical data are available.

## 1 Introduction

Antiretroviral agents are among the therapeutic agents with the highest potential for drug–drug interactions (DDIs), mainly due to their inhibitory and/or inductive effects on liver-metabolizing enzymes such as the cytochrome P450 (CYP) isoenzymes and drug transporters [1, 2]. Studies assessing the prevalence of DDIs with HIV therapy have indeed shown that potential clinically significant DDIs are common, affecting 19–41 % of HIV-infected patients [3–7]. The problem of DDIs is likely to worsen with an aging HIV patient population where multiple treatments for co-morbidities may interact with HIV therapy [8]. DDIs may be associated with a substantial risk for toxicity or decreased efficacy and therefore the management of DDIs is crucial for the care of HIV-infected patients.

One of the current issues related to DDIs is the limited availability of clinical data on DDIs between antiretroviral drugs and commonly prescribed drugs in HIV patients. In the absence of clinical data, potential clinically relevant DDIs are predicted based on in vitro experimental data which may not correctly reflect the in vivo drug metabolism (especially if these data are not considered in models to predict DDI). For instance, the contribution of a given CYP to the overall metabolic clearance (CL) is not always scaled to the hepatic CYP expression. In addition, the concentrations of drug substrates and inhibitors/inducers used in vitro may not always reflect the therapeutic concentrations to which CYP are exposed. Finally, these experimental data do not incorporate the concurrent inhibitory and inducing effects on CYPs. Therefore, the net effect of a DDI can be difficult to predict, particularly for drugs whose metabolism can be simultaneously induced and inhibited by a given DDI perpetrator.

Efavirenz, a first-generation non-nucleoside reverse transcriptase inhibitor, is a well-known perpetrator of DDIs. Efavirenz is primarily metabolized by CYP2B6 to 8-hydroxy-efavirenz (8-hydroxy-EFV), secondarily by CYP2A6 to 7-hydroxy-efavirenz (7-hydroxy-EFV) and by uridine 5'-diphospho-glucuronosyltransferase (UGT) 2B7 [9, 10]. Efavirenz has been shown to be an inducer of CYP3A4 and CYP2B6 in vivo [11, 12] but also an inhibitor of CYP2C8 in vitro [13]. The clinical relevance of CYP2C8 inhibition by efavirenz has also been demonstrated in a report describing an increase in amodiaquine exposure, a CYP2C8 substrate, and related hepatotoxicity during co-administration with efavirenz in healthy volunteers [14]. The net effect of efavirenz on dual CYP3A4/CYP2C8 substrates is currently unknown and difficult to predict when considering in vitro drug metabolism data alone.

Physiologically based pharmacokinetic (PBPK) modeling has emerged as a performant tool in recent years for prediction of CYP-mediated DDIs [15, 16]. This approach enables the simulation of the pharmacokinetics of a drug using in vitro drug data (i.e., physicochemical characteristics, intrinsic CL [$CL_{int}$], permeability) through a mathematical description of absorption, distribution, metabolism, and elimination (ADME) of a drug. The in vitro $CL_{int}$ is usually quantified using recombinant CYPs and subsequently scaled up to determine the hepatic CL by considering factors such as CYP abundance in microsomal protein, microsomal protein per gram of liver, liver weight, blood flow, and protein binding. The magnitude of a DDI is simulated using data from in vitro studies investigating the potential of a given drug to inhibit or induce CYPs. These data are subsequently integrated in the equations describing reverse or time-dependent inhibition or induction. The PBPK modeling approach presents the advantage of integrating the fraction of the drug metabolized by a given CYP and the effect of concurrent inhibition and induction of multiple CYPs. In addition, this approach incorporates gut metabolism ($F_g$) and the temporal changes in the concentration of the perpetrator and victim drugs and therefore predicts DDI in a more comprehensive and meaningful way [17]. Finally, PBPK models can be applied to simulate clinical scenarios in relation to DDIs to provide guidance on how to manage DDIs for drug combinations used in clinical practice but for which limited clinical data are available [18, 19].

The aim of this study was to develop PBPK models integrating concurrent inducing and inhibitory effects to simulate the magnitude of DDIs between efavirenz and dual CYP3A4/CYP2C8 substrates with distinct contributions of CYP3A4 versus CYP2C8 to their overall metabolism. The models were first applied to simulate the pharmacokinetics of individual drugs and validated against available clinical data to evaluate their predictive performance. The models were subsequently used to simulate virtual DDI trials to determine the magnitude of DDIs and the potential dose adjustments to overcome the effect of efavirenz on various dual CYP3A4/CYP2C8 substrates.

## 2 Methods

### 2.1 Parameters of Physiologically Based Pharmacokinetic (PBPK) Models

The PBPK models were designed using Simbiology® version 4.3.1, a product of MATLAB® version 8.2 (MathWorks, Natick, MA, USA; 2013). The main parameters of the models are described following.

#### 2.1.1 Virtual Individuals

Virtual individuals were generated using a population physiology model (*physB*) which compiles a statistical description of the physiological and anatomical parameters representing the general adult population (age range of 18–60 years with a mean age of 36.5 ± 13 years) [20]. Age, body surface area, body mass index, weight, and height were used to allometrically scale organ and tissue weights. The blood circulation took into account the cardiac output and the regional blood flows to the organs as previously described [20].

#### 2.1.2 Oral Absorption

Oral absorption was simulated using a compartmental absorption and transit model and considering a stomach transit time of 0.5 h and a small intestine transit time of 3.3 h as previously reported [21]. The absorption rate constant ($k_a$) of drugs was derived from the effective permeability ($P_{eff}$) obtained from published Caco-2 cells or, when these data were not available, from polar surface area and hydrogen bond donor experimental data as previously described [22]. The absorption model does not handle a solid dosage form and therefore assumes no limitation from solubility.

#### 2.1.3 Intestinal Metabolism

The CL of drugs in the gut ($CL_g$) was determined by considering the abundance of CYP3A in the intestinal tissue (AbCYP3A) and the in vitro $CL_{int}$ as described previously [22, 23]. The $CL_g$ did not incorporate efavirenz induction effect on intestinal CYP3A since in vivo studies have shown that efavirenz does not induce intestinal enzymes or transporters [12, 24]. The well-stirred gut model, assuming instant distribution of the drug to the enterocytes, was used to determine the amount of drug escaping $F_g$ and reaching the liver using the following equation (Eq. 1) (it is of note that comparable $F_g$ values were obtained when using the $Q_{gut}$ model):

$$F_g = \frac{Q_g}{Q_g + f_{u,g} \times CL_g}, \quad (1)$$

where $Q_g$ and $f_{u,g}$ represent the blood flow to the gut and the fraction of the drug unbound in the gut, respectively.

#### 2.1.4 Hepatic Metabolism

The total $CL_{int}$ ($TotCL_{int}$) of a given CYP in the liver was determined by considering the in vitro $CL_{int}$, the amount of CYP (AbCYP) present in a milligram of microsomal protein per gram liver (MPPGL), and the liver weight as described previously [23]. The following equation (Eq. 2) was used to calculate the age-related values of MPPGL as previously reported by Barter et al. [25]:

$$MPPGL = 10^{1.407 + 0.0158 \times Age - 0.00038 \times Age2 + 0.0000024 \times Age3}. \quad (2)$$

Efavirenz induction (Ind) and inhibition (Inh) of liver enzymes was integrated in the calculation of individual $TotCL_{int}$ using the following equations (Eqs. 3 and 4):

$$Ind = 1 + \frac{E_{max} \times I_h}{EC_{50} + I_h}, \quad (3)$$

$$Inh = 1 + \frac{I_h}{K_i}, \quad (4)$$

where $E_{max}$, $EC_{50}$, $K_i$, and $I_h$ represent the maximum induction (net maximum fold increase), concentration of inducer producing 50 % of $E_{max}$, concentration of inhibitor producing 50 % of maximum inhibition, and the concentration of inducer/inhibitor in the liver tissue, respectively.

The total liver $CL_{int}$ ($CL_{liver}$) was subsequently calculated as the sum of all the $TotCL_{int}$ of enzymes contributing to the metabolism of a given drug as described previously [22]. Finally, the systemic CL was determined taking into account the blood flow to the liver ($Q_h$) as detailed thereafter (Eq. 5):

$$CL = \frac{Q_h \times f_u \times CL_{liver}}{Q_h + f_u \times CL_{liver}}, \quad (5)$$

where $f_u$ is the fraction unbound in blood.

The amount of drug escaping hepatic metabolism ($F_h$) and reaching the systemic circulation was computed using the following equation (Eq. 6):

$$F_h = \frac{Q_h}{Q_h + f_u \times CL_{liver}}. \quad (6)$$

#### 2.1.5 Distribution

The volume of distribution was simulated by calculating the tissue to plasma partition coefficient for each organ and considering organ volumes originated from *physB* using previously published equations [26, 27].

#### 2.1.6 Intravenous Drug Administration

A compartment was created for the intravenous drug administration in order to simulate the direct release of the drug in the arterial compartment. The release rate was set to reach complete administration of the drug in 2 h in order to reflect the perfusion time.

### 2.2 Parameters of Simulated Drugs

PBPK models were developed using published in vitro data for the following compounds: efavirenz (DDI perpetrator), the dual CYP3A4/CYP2C8 substrates repaglinide, montelukast, pioglitazone, and paclitaxel, and the CYP3A4 substrate maraviroc to validate efavirenz inducing effect on CYP3A4.

The in vitro data describing the physicochemical parameters and the metabolism of the drugs by different recombinant enzyme isoforms are summarized in Table 1. Efavirenz is mainly hydroxylated to 8-hydroxy-EFV by CYP2B6 and to a lesser extent by CYP2A6, CYP1A2, CYP3A4, and CYP3A5. The conversion to 7-hydroxy-EFV by CYP2A6 and glucuronidation by UGT2B7 represents minor pathways [9, 10]. Efavirenz induces CYP3A4 and CYP2B6 [18] and inhibits CYP2C8, CYP2C9, and CYP3A4 [13]. CYP3A4/CYP2C8 substrates were selected to have a distinct contribution of CYP3A4 versus CYP2C8 to their overall metabolism based on in vitro drug metabolism data. The antidiabetic repaglinide is metabolized equally by CYP3A4 and CYP2C8 [28]; the bronchodilator montelukast and the antidiabetic pioglitazone are metabolized to a larger extent by CYP2C8 than by CYP3A4 [29, 30]; and the anticancer agent paclitaxel is metabolized primarily by CYP2C8 with a minor contribution of CYP3A4 [31]. The minor contribution of CYP2C9 to montelukast metabolism and the inhibitory effect of efavirenz on CYP2C9 were also integrated in the montelukast PBPK model. None of the evaluated CYP3A4/CYP2C8 substrates have clinically relevant inhibitory or inducing effects on CYPs and therefore are not expected to impact efavirenz. The antiretroviral agent maraviroc, a substrate of CYP3A4 devoid of inhibitory or inducing effects on CYPs, was selected to validate the strength of CYP3A4 induction by efavirenz [32]. Repaglinide, paclitaxel, and maraviroc are substrates of the hepatic transport organic anion-transporting polypeptide (OATP) 1B1 [33–35]; however, this transporter was not integrated in the models since efavirenz has been shown to have no effect on OATP1B1 [24]. Finally, all drugs considered in this study are extensively metabolized in the liver and therefore no renal CL component was included in the simulations.

### 2.3 Validation of PBPK Models

In order to assess and validate the models, the simulated pharmacokinetic profiles of individual drugs were compared against existing clinical data [36–40]. In addition, the strength of CYP3A4 induction by efavirenz was validated by comparing the simulated versus observed DDI between maraviroc and efavirenz [32]. The strength of CYP2C8 inhibition by efavirenz could not be validated due to limited data from clinical DDI studies.

### 2.4 Design of Virtual Drug–Drug Interaction (DDI) Studies

The dosage and frequency of administration of the evaluated drugs were selected to reflect clinical practice and data from clinical studies used to validate the models. Simulations were performed in 50 virtual individuals receiving oral repaglinide 2 mg three times daily, montelukast 10 mg once daily, or pioglitazone 15 mg once daily without efavirenz for 14 days followed by co-administration with efavirenz 600 mg once daily for another 14 days. Paclitaxel is administered intravenously at a dose of 175 mg/m$^2$ every 3 weeks. Therefore, paclitaxel simulations were performed by creating a compartment to reflect the intravenous drug administration and the dose was multiplied by the body surface area. Similarly to the other drugs, simulations were performed for paclitaxel alone and in combination with efavirenz. Additional simulations were performed to determine dose adjustments of repaglinide, montelukast, pioglitazone, and paclitaxel to overcome the DDIs with efavirenz. The criterion for dose adjustments was to obtain a value of drug exposure as close as possible to the exposure of the drug administered alone considering available drug dosages on the market (including the possibility to split a tablet as for pioglitazone) in order to provide realistic dosage adjustments.

**Table 1** Physicochemical and metabolic characteristics of simulated drugs

| Parameter | Efavirenz | | Repaglinide | Montelukast | Pioglitazone | Paclitaxel | Maraviroc |
|---|---|---|---|---|---|---|---|
| Physicochemical properties [52, 53] | | | | | | | |
| Molecular weight | 315.7 | | 452.6 | 586.2 | 356.4 | 853.9 | 513.7 |
| Log *Po*:w | 4.6 | | 3.95 | 7.9 | 2.3 | 3.54 | 2.4 [54] |
| p*Ka* | 10.2 | | 4.19 | 4.4 | 5.6 | 10.36 | 7.3 [54] |
| $f_u$ | 0.015 | | 0.03 | 0.0018 | 0.015 | 0.03 [55] | 0.13 [56] |
| B/P | 0.74 | | 0.62 | 0.65 [29] | 1.0 | 0.5 | 0.59 [54] |
| PSA | 38.33 | | 78.87 | 70.42 | 68.29 | 221.29 | 63.05 |
| HBD | 1 | | 2 | 2 | 1 | 4 | 1 |
| Absorption | | | | | | | |
| Caco-2 $P_{app}$ | $2.5 \times 10^{-6}$ [18] | | $26.1 \times 10^{-6}$ [33] | $1.5 \times 10^{-6}$ [57] | | $0.36 \times 10^{-6}$ [58] | |
| Metabolism | | | | | | | |
| CYP1A2 $CL_{int}$ | 0.07 [10] | | | | | | |
| CYP2A6 $CL_{int}$ | 0.08 [10] | | | | | | |
| CYP3A4 $CL_{int}$ | 0.007 [10] | | 1.8 [43] | 1.8 [29] | 0.3 [39] | 0.19 [44] | 1.7 [54] |
| CYP3A5 $CL_{int}$ | 0.03 [10] | | | | | | |
| CYP2B6 $CL_{int}$ | 0.55 [10] | | | | | | |
| CYP2C8 $CL_{int}$ | | | 1.7 [43] | 3.6 [29] | 0.9 [39] | 1.68 [31] | |
| CYP2C9 $CL_{int}$ | | | | 0.48 [29] | | | |
| Elimination | | | | | | | |
| $f_e$ [59–64] | <0.01 | | 0.001 | <0.002 | Negligible | 0.013–0.126 | 0.08 |
| CYP inhibition ($K_i$) | | | | | | | |
| CYP3A4 | 40.3 [13] | | | | | | |
| CYP2C8 | 4.8 [13] | | | | | | |
| CYP2C9 | 19.5 [13] | | | | | | |
| CYP induction | $E_{max}$ | $EC_{50}$ | | | | | |
| CYP3A4 | 6.5 [18] | 3.9 [18] | | | | | |
| CYP2B6 | 5.7 [18] | 0.8 [18] | | | | | |

*B/P* blood to plasma drug ratio, $CL_{int}$ intrinsic clearance expressed as µL/min/pmol, *CYP* cytochrome P450, $EC_{50}$ concentration of inducer producing 50 % of maximum induction expressed as µmol/L, $E_{max}$ maximum induction, $f_e$ fraction of drug excreted unchanged in urine, $f_u$ fraction of drug unbound in blood, *HBD* number of hydrogen bond donors, $K_i$ concentration of inhibitor producing 50 % of maximum inhibition expressed as µmol/L, *log Po:w* partition coefficient between octanol and water, $P_{app}$ drug permeability from apical to basolateral in Caco-2 cell monolayer ($10^{-6}$ cm/s), *pKa* acid dissociation constant, *PSA* polar surface area

The pharmacokinetic parameters of the simulations were presented as mean ± standard deviation (SD). The area under the plasma concentration–time curve (AUC) for a dosing interval ($AUC_\tau$) and maximum concentration ($C_{max}$) were evaluated after logarithmic transformation, providing point estimates and 90 % confidence intervals (CIs) for the combined/single drug administration ratio.

## 3 Results

### 3.1 Validation of the PBPK Models

The pharmacokinetics at steady state were initially simulated for each drug alone in order to evaluate the performance of PBPK models. As summarized in Table 2, the simulated pharmacokinetic parameters of efavirenz, repaglinide, montelukast, pioglitazone, and paclitaxel were in good accordance with previously described clinical data. The models could predict the AUC and $C_{max}$ of all drugs within a twofold difference of the observed corresponding pharmacokinetic parameters (Fig. 1a, b) and therefore predictions were within the commonly agreeable limits of variability for validation considering the variability in the observed pharmacokinetic parameters of some drugs [41].

Furthermore, the simulated DDI between efavirenz (600 mg once daily) and the CYP3A4 substrate maraviroc (100 mg twice daily) gave results comparable to those described in a clinical trial [32]. The comparison of the maraviroc $AUC_\tau$ with and without efavirenz gave a geometric mean ratio [GMR] (90 % CI) of 0.36 (0.31–0.68) for the simulation compared with 0.49 (0.41–0.57) for the

**Table 2** Validation of physiologically based pharmacokinetic models: simulated versus observed clinical data from the literature

| Drug | $AUC_\tau$ (ng · h/mL) | $C_{max}$ (ng/mL) | $F$ (%) | CL (L/h) | $V_d$ (L) | References |
|---|---|---|---|---|---|---|
| Efavirenz 600 mg od | | | | | | |
| Simulated | 88,153 ± 40,674 | 5631 ± 1703 | 73 | 6.8 ± 2.5[a] | 67 ± 10[b] | [36, 65] |
| Observed | 57,592 ± 22,849 | 4037 ± 1158 | NA | 9.4[a] | 252[b] | |
| Repaglinide 2 mg tid | | | | | | |
| Simulated | 55 ± 27 | 20.3 ± 7.3 | 70 | 43 ± 11 | 29 ± 4 | [37, 59] |
| Observed | 69 ± 78 | 47.9 ± 32.0 | 62.5 | 38 ± 16 | 31 ± 12 | |
| Montelukast 10 mg od | | | | | | |
| Simulated | 2781 ± 914 | 352 ± 60 | 81 | 4.8 ± 1.3 | 14 ± 1.4 | [38, 66] |
| Observed | 3940 ± 880 | 470 ± 120 | 66 | 2.7 | 10.5 | |
| Pioglitazone 15 mg od | | | | | | |
| Simulated | 3281 ± 1161 | 488 ± 72 | 92 | 5.0 ± 1.4[a] | 19.0 ± 1.5[b] | [39, 61] |
| Observed | 5020 ± 1070 | 597 ± 115 | >80 | 5–7[a] | 17.5[b] | |
| Paclitaxel 175 mg/m$^2$ iv | | | | | | |
| Simulated | 18,895 ± 7015 | 4680 ± 730 | 100 | 38 ± 11 | 38 ± 5 | [40, 67] |
| Observed | 16,045 (21 %) | 3980 (35 %) | 100 | 21.2 | 137 | |

Data are given as arithmetic mean ± SD or geometric mean (% coefficient of variation)

$AUC_\tau$ area under the plasma concentration–time curve over a dosing interval, *CL* clearance, $C_{max}$ maximum plasma concentration, *F* absolute bioavailability, *iv* intravenous administration, *NA* not available, *od* once daily, *tid* three times daily, $V_d$ volume of distribution for an adult body weight of 70 kg

[a] Apparent clearance (CL/*F*)

[b] Apparent volume of distribution ($V_d$/*F*)

observed clinical data. Similarly, comparison of the maraviroc $C_{max}$ with and without efavirenz gave a GMR of 0.39 (0.34–0.44) for the simulation compared with 0.43 (0.30–0.62) for the observed data, indicating that the strength of CYP3A4 induction by efavirenz was relatively well-represented by the PBPK models.

### 3.2 Simulations of DDIs between Efavirenz and Cytochrome P450 (CYP) 3A4/CYP2C8 Substrates

The simulated DDIs between efavirenz and CYP3A4/CYP2C8 substrates are presented as GMR (90 % CI) of the $AUC_\tau$ and $C_{max}$ for the combined/single drug administration ratio (Table 3). These data were further dissected to look at the effect of efavirenz on the systemic CL, intestinal metabolism ($F_g$) and hepatic metabolism $F_h$ of individual CYP3A4/CYP2C8 substrates.

The simulation of repaglinide plasma profile at a dose of 2 mg three times daily was characterized by a mean bioavailability of 0.70 (Table 2) resulting mainly from a low intestinal metabolism ($F_g = 0.98$) and a first-pass metabolism ($F_h = 0.71$. The systemic CL was equal to 43 L/h, with CYP3A4 and CYP2C8 contributing to 80 and 20 % of the overall systemic CL, respectively. Efavirenz concurrent induction of CYP3A4 and inhibition of CYP2C8 caused an overall inducing effect on repaglinide exposure with a substantial effect on $F_h$ and systemic CL. Efavirenz increased repaglinide hepatic metabolism by 40 % ($F_h$ decreased from 0.71 to 0.43) and CL increased to 77 L/h. This had a major effect on repaglinide pharmacokinetics, reducing $AUC_\tau$ by 65 % and $C_{max}$ by 60 % (Table 3). Efavirenz had no effect on $F_g$. Dose adjustment simulations showed that a dose of repaglinide 5 mg three times daily resulted in a mean (±SD) AUC of 65 ± 54 (observed repaglinide AUC when administered alone at 2 mg three times daily: 69 ± 78), which was sufficient to overcome the effect of efavirenz on repaglinide exposure (Table 3; Fig. 2a).

The simulation of montelukast (10 mg once daily) pharmacokinetics gave a mean bioavailability of 0.81 as a result of 16 % of the dose not absorbed (fraction absorbed [$F_a$] = 0.84), low intestinal metabolism ($F_g = 0.99$) and low hepatic metabolism ($F_h = 0.97$). Montelukast is a low hepatic extraction drug with an estimated systemic CL equal to 4.8 L/h that is mediated by CYP3A4 (3.2 L/h), CYP2C8 (1.4 L/h), and CYP2C9 (0.2 L/h). Efavirenz concurrent induction of CYP3A4 and inhibition of CYP2C8 and CYP2C9 caused an overall reduction of montelukast $AUC_\tau$ and $C_{max}$ by 40 and 23 %, respectively (Table 3). Efavirenz had a modest effect on $F_h$ (5 % reduction from 0.97 to 0.92), as expected for low hepatic extraction drugs. Co-administration with efavirenz increased CL to 12.1 L/h mainly by increasing CYP3A4 CL to 11.8 L/h, whereas CL by CYP2C8 and CYP2C9 were reduced to 0.2 and 0.1 L/h, respectively. A dose increase to montelukast 14 mg once daily resulted in a

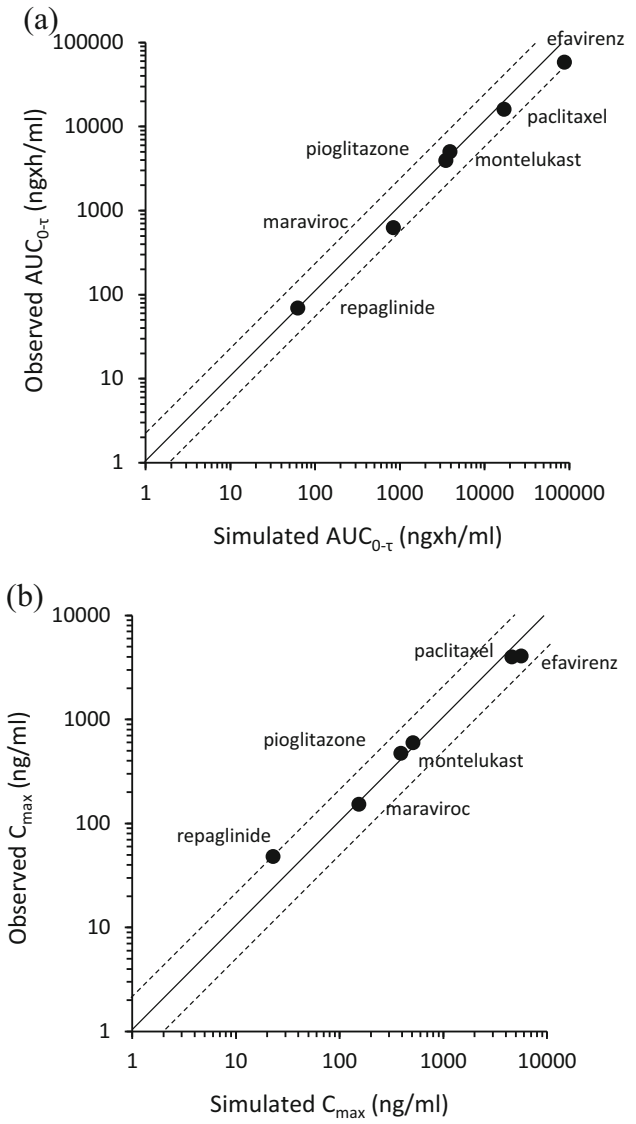


**Fig. 1** Scatter plots representing the simulated versus observed area under the plasma concentration–time curve over a dosing interval ($AUC_\tau$) (**a**) and maximum concentration ($C_{max}$) (**b**) for all drugs evaluated in the study. The simulated values represent the mean value of 50 simulations obtained at steady-state administration for repaglinide 2 mg three times daily; montelukast 10 mg once daily; pioglitazone 15 mg once daily; paclitaxel 175 mg/m$^2$; maraviroc 100 mg twice daily; and efavirenz 600 mg once daily given alone. The *dashed lines* represent a twofold difference from the observed pharmacokinetic parameters

mean AUC of 2293 ± 980 (observed montelukast AUC when administered alone at 10 mg once daily: 3940 ± 880), which was sufficient to overcome the efavirenz effect on montelukast exposure (Table 3; Fig. 2b).

The simulated pharmacokinetics of pioglitazone (15 mg once daily) gave a mean total systemic CL of 4.5 L/h, which was mediated by CYP3A4 (2.7 L/h) and CYP2C8 (1.8 L/h). The bioavailability was equal to 0.92 and resulted from a good absorption of the drug ($F_a = 0.96$), minimal $F_g$ (0.99), and low $F_h$ (0.96). Efavirenz induction of CYP3A4 increased its CL to 11.6 L/h while the inhibitory effect on CYP2C8 reduced its CL to 0.26 L/h, which resulted in a mean total systemic CL equal to 11.9 L/h. The overall effect was a reduction of pioglitazone $AUC_\tau$ and $C_{max}$ by 45 and 27 %, respectively (Table 3). Efavirenz had a minor effect on $F_h$ with a 6 % reduction in $F_h$ (from 0.96 to 0.90). A dose increase to pioglitazone 22.5 mg once daily (representing 1.5 tablets dosed at 15 mg) resulted in a mean AUC of 3170 ± 1635 (observed pioglitazone AUC when administered alone at 15 mg once daily: 5020 ± 1070), which was sufficient to overcome the effect of efavirenz on pioglitazone exposure (Table 3; Fig. 2c).

Paclitaxel (175 mg/m$^2$) total CL was simulated as being 38 L/h, with CYP3A4- and CYP2C8-mediated metabolism contributing to 30 and 70 % of the overall systemic CL, respectively. Efavirenz concurrent induction of CYP3A4 and inhibition of CYP2C8 caused a modest change in paclitaxel exposure with a 14 % decrease in $AUC_\tau$ and 9 % reduction in $C_{max}$ (Table 3). Efavirenz increased total CL to 54 L/h and the $F_h$ of paclitaxel by 17 %. Given the small magnitude of the interaction with efavirenz, no dosage adjustment was required for paclitaxel when co-administered with efavirenz (Table 3; Fig. 2d).

## 4 Discussion

The management of DDIs remains an important aspect of the care of HIV-infected patients. Due to the limited number of clinical DDI studies between antiretroviral drugs and commonly prescribed co-medications, DDIs are often predicted based on the metabolic pathway of individual drugs. However, predictions can be difficult, particularly when DDI perpetrators are simultaneously inducing and inhibiting multiple CYPs. The PBPK modeling approach was used to predict the magnitude of DDIs between efavirenz, an inducer of CYP3A4 and inhibitor of CYP2C8, and several dual CYP3A4/CYP2C8 substrates.

PBPK models were developed to include the contribution of each individual CYP to the overall metabolic CL of the drug and subsequently scaled to their hepatic expression. For CYP2C8, scaling to the hepatic content considered a mean CYP2C8 protein expression of 31 ± 18 pmol/mg as previously described [42] and the fact that CYP2C8 accounts for 6–7 % of the total hepatic CYP content. Furthermore, the models integrated the simultaneous inducing and inhibitory effects on CYP3A4 and CYP2C8 as well as the temporal changes in the concentration of efavirenz and the dual CYP3A4/CYP2C8 substrates in order to best reflect the in vivo situation. The developed models were able to predict correctly the pharmacokinetic

**Table 3** Simulated magnitude of drug–drug interactions between efavirenz and cytochrome P450 3A4/2C8 substrates and dosage adjustments to overcome the interaction with efavirenz

| Parameter | $AUC_\tau$ GMR (90 % CI) | $C_{max}$ GMR (90 % CI) |
|---|---|---|
| Repaglinide (2 mg tid) + EFV | 0.35 (0.30–0.42) | 0.40 (0.35–0.46) |
| Repaglinide (2 mg tid) alone | | |
| Repaglinide (5 mg tid) + EFV | 1.01 (0.83–1.20) | 1.11 (0.95–1.29) |
| Repaglinide (2 mg tid) alone | | |
| Montelukast (10 mg od) + EFV | 0.60 (0.53–0.68) | 0.77 (0.72–0.82) |
| Montelukast (10 mg od) alone | | |
| Montelukast (14 mg od) + EFV | 0.79 (0.70–0.89) | 1.07 (1.00–1.14) |
| Montelukast (10 mg tid) alone | | |
| Pioglitazone (15 mg od) + EFV | 0.55 (0.48–0.63) | 0.73 (0.68–0.77) |
| Pioglitazone (15 mg od) alone | | |
| Pioglitazone (22.5 mg od) + EFV | 0.91 (0.81–1.05) | 1.15 (1.07–1.23) |
| Pioglitazone (15 mg od) alone | | |
| Paclitaxel (175 mg/m$^2$) + EFV | 0.86 (0.76–0.96) | 0.91 (0.86–0.96) |
| Paclitaxel (175 mg/m$^2$) alone | | |

*$AUC_\tau$* area under the plasma concentration–time curve over a dosing interval, *CI* confidence interval, *$C_{max}$* maximum plasma concentration, *EFV* efavirenz, *GMR* geometric mean ratio, *od* once daily, *tid* three times daily

parameters of individual drugs. The simulations showed that the net effect of efavirenz on dual CYP3A4/CYP2C8 substrates was induction of metabolism, which was predicted to be weak to moderate depending on the contribution of CYP2C8 to the overall metabolic CL as illustrated for the intermediate hepatic extraction drugs—repaglinide and paclitaxel. Repaglinide has been shown in vitro to be equally metabolized by CYP3A4 and CYP2C8 [43], whereas CYP2C8 is the major contributor of paclitaxel metabolism [31, 44]. The simulations showed that the co-administration of efavirenz increased the $F_h$ of repaglinide by 40 % and only by 17 % for paclitaxel. This difference can be explained by the lower fraction of CYP3A4 metabolism being induced by efavirenz in the case of paclitaxel since CYP2C8 metabolism is the major contributor of paclitaxel overall $F_h$, whereas CYP3A4 is the major contributor of repaglinide metabolism. This results in paclitaxel total CL being increased from 38 L/h (without efavirenz) to 54 L/h (with efavirenz), whereas repaglinide total CL went from 43 L/h (without efavirenz) to 77 L/h (with efavirenz). Although repaglinide and paclitaxel are substrates of the hepatic transporter OATP1B1 [33, 35], this transporter was not included in the models since in vivo data indicate that it is not impacted by efavirenz [24]. However, since hepatic uptake by OATP1B1 is the rate-determining step in the CL of these drugs and since the transporter capacity can be saturated, we cannot exclude that induction might have been over-predicted by not including OATP1B1 in our models.

Clinical data from DDI studies have shown that DDIs with repaglinide can be complex. For instance, rifampicin (rifampin), a strong inducer of CYP3A4 and to a lesser extent of CYP2C8, but also an inhibitor of OATP1B1, was shown to reduce the repaglinide AUC by 50 % when administered simultaneously. However, when repaglinide was given 24 h after the last rifampicin dose, the repaglinide AUC decreased by 80 % [45]. The lower magnitude of the DDI observed for the simultaneous administration of drugs has been attributed to the concomitant inhibitory effect of rifampicin on OATP1B1, which limits the amount of repaglinide entering the liver and subsequently being induced by CYP3A4. However, when repaglinide was given 24 h after rifampicin, the inhibitory effect on OATP1B1 was no longer present and therefore the DDIs reflected only the inducing effect on CYPs [45]. Efavirenz has no limiting effect on the entry of repaglinide in the liver, which could explain that the simulated induction of repaglinide is comparable with the one observed when repaglinide is given simultaneously to rifampicin even though efavirenz is a less potent inducer of CYPs. Few clinical DDI studies are available for paclitaxel; however, data have shown that co-administration with the strong CYP3A4 inhibitor ketoconazole did not impact paclitaxel exposure [46]. This observation is consistent with our simulation showing a minimal effect of efavirenz on paclitaxel exposure. Our simulation also suggest that the efavirenz inducing effect on CYP3A4 is stronger than the inhibitory effect on CYP2C8; although paclitaxel was predominantly cleared by CYP2C8, its exposure was not increased by efavirenz. The assumption of a moderate inhibitory effect of efavirenz on CYP2C8 is consistent with a report indicating that concomitant use of efavirenz increased amiodaquine exposure by twofold in one patient and fourfold in another patient [14]. As a

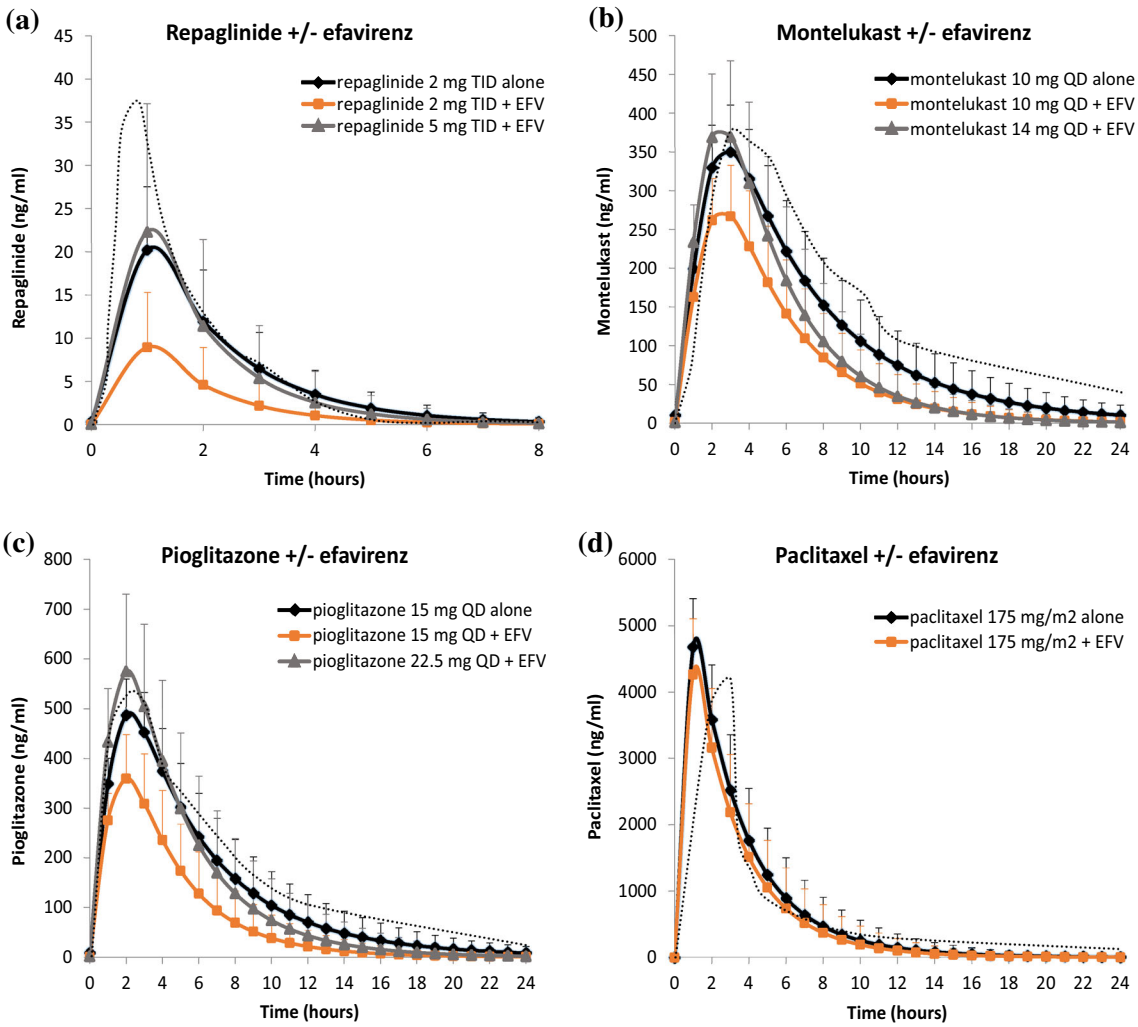


**Fig. 2** Simulated steady-state plasma profile of repaglinide (**a**), montelukast (**b**), pioglitazone (**c**), and paclitaxel (**d**) administered alone (*black profile*) and together with multiple doses of efavirenz (*orange profile*). The plasma profile after adjustment of the dosage to overcome the interaction with efavirenz is represented in *grey*. Predicted profiles are represented as mean ± standard deviation. The *dashed lines* represent the observed plasma profiles of repaglinide 2 mg three times daily [37], montelukast 10 mg once daily [38], pioglitazone 15 mg once daily [39], and paclitaxel 175 mg/m$^2$ [40]. *EFV* efavirenz, *QD* once daily, *TID* three times daily

comparison, the strong CYP2C8 inhibitor gemfibrozil is predicted to increase the exposure of amiodarone, a drug exclusively metabolized by CYP2C8, by >15-fold [47].

In vitro studies have shown that montelukast and pioglitazone are mainly metabolized by CYP2C8 [29, 39]. This has been corroborated by data from clinical DDI studies showing that gemfibrozil increased montelukast exposure by fivefold [48] as a result of CYP2C8 inhibition only since montelukast is not transported by OATP1B1 [49]. Inhibition of CYP3A4 has led to discordant results as itraconazole was shown to have no significant effect on montelukast exposure [49], whereas clarithromycin was shown to increase montelukast exposure by 2.4-fold in volunteers [38]. Our simulation showed that efavirenz reduced montelukast exposure, suggesting an effect on CYP3A4. Finally, available clinical DDI studies for pioglitazone showed that rifampicin reduced the pioglitazone AUC by 54 % [50]. Similarly, our simulation showed a reduced pioglitazone exposure although, comparative to rifampicin, the magnitude of the efavirenz effect might be slightly overestimated as our models were shown to produce a more pronounced inducing effect on the AUC when looking at the efavirenz–maraviroc DDI. The stronger induction of CYP3A4 in our model could be explained by the higher simulated versus observed efavirenz AUC.

Several limitations to our modeling approach should be acknowledged. The strength of efavirenz CYP2C8 inhibition could not be validated due to limited data from clinical DDI studies. Furthermore, the exact role of CYP2C8 in the observed DDIs is difficult to determine since available DDI studies were performed with no fully selective in vivo inhibitors or inducers of CYP2C8 (i.e., rifampicin,

gemfibrozil). Furthermore, all evaluated CYP2C8 substrates in previous clinical studies were partially metabolized by other enzymes or were substrates of OATP1B1, further complicating the interpretation of DDI studies. Also, our models did not take into account the effect of genetic variations on CYP2C8 activity, which may also have an impact on the magnitude of DDIs [51]. Finally, our models did not incorporate the physiological changes related to aging and therefore the magnitude of the simulated DDI does not reflect what might be observed in elderly patients.

## 5 Conclusion

The developed PBPK models were able to predict the pharmacokinetics of efavirenz and dual CYP3A4/CYP2C8 substrates. Furthermore, the models, integrating mixed effects on CYPs, showed that the net effect of efavirenz on dual CYP3A4/CYP2C8 substrates was induction of metabolism. However, the magnitude of induction tended to be less pronounced for dual CYP3A4/CYP2C8 substrates with predominant CYP2C8 metabolism, which was explained by a lower fraction of CYP3A4 metabolism being induced by efavirenz. The PBPK modeling approach constitutes a useful mechanistic approach for the quantitative prediction of DDIs. This approach is of particular interest for the management of DDIs with HIV therapy given that several antiretroviral drugs are characterized by concurrent inducing and inhibitory effects on CYPs (i.e., darunavir/ritonavir, lopinavir/ritonavir, tipranavir/ritonavir), which makes prediction of DDIs difficult, especially in the context of an aging, poly-medicated HIV population. Importantly, this approach can be applied to simulate a virtual clinical study scenario in order to characterize DDIs for drug combinations used in daily clinical practice but for which limited clinical data are available, and thus might be useful in providing guidance on how to manage DDIs. Other applications of great clinical interest for HIV therapy include the use of PBPK modeling to predict the pharmacokinetics in special populations such as the elderly, children, or pregnant women by developing models that integrate the physiological changes related to these conditions and thus optimize the treatment strategies.

**Compliance with Ethical Standards**

CM has been supported by a Grant of the University of Basel (Grant DMS2265) and has received educational Grants from AbbVie, Gilead, and Bristol-Myers-Squibb for her clinical service on drug–drug interactions, and research funding from Janssen. DB has received research Grants from Merck, AbbVie, Gilead, ViiV, Bristol-Myers-Squibb, and Janssen, and travel bursaries from Gilead, ViiV, AbbVie, and Janssen. MS has received research funding from ViiV and Janssen. LE, MB, and RR declare no conflicts of interest.

## References

1. Barry M, Mulcahy F, Merry C, Gibbons S, Back D. Pharmacokinetics and potential interactions amongst antiretroviral agents used to treat patients with HIV infection. Clin Pharmacokinet. 1999;36(4):289–304.
2. Marzolini C, Battegay M, Back D. Mechanisms of drug interactions II: transport proteins. In: Piscitelli SC, Rodvold KA, Pai MP, editors. Drug interactions in infectious diseases. Totawa: Humana Press; 2011. p. 43–72.
3. Evans-Jones JG, Cottle LE, Back DJ, Gibbons S, Beeching NJ, Carey PB, et al. Recognition of risk for clinically significant drug interactions among HIV-infected patients receiving antiretroviral therapy. Clin Infect Dis. 2010;50(10):1419–21.
4. Marzolini C, Elzi L, Gibbons S, Weber R, Fux C, Furrer H, Swiss HIV Cohort Study, et al. Prevalence of comedications and effect of potential drug-drug interactions in the Swiss HIV Cohort Study. Antivir Ther. 2010;15(3):413–23.
5. Seden K, Merry C, Hewson R, Siccardi M, Lamorde M, Byakika-Kibwika P, et al. Prevalence and type of drug-drug interactions involving ART in patients attending a specialist HIV outpatient clinic in Kampala, Uganda. J Antimicrob Chemother. 2015;70(12):3317–22.
6. Kigen G, Kimaiyo S, Nyandiko W, Faragher B, Sang E, Jakait B, et al. Prevalence of potential drug-drug interactions involving antiretroviral drugs in a large Kenyan cohort. PLoS One. 2011;6(2):e16800.
7. de Maat MM, de Boer A, Koks CH, Mulder JW, Meenhorst PL, van Gorp EC, et al. Evaluation of clinical pharmacist interventions on drug interactions in outpatient pharmaceutical HIV-care. J Clin Pharm Ther. 2004;29(2):121–30.
8. Marzolini C, Back D, Weber R, Furrer H, Cavassini M, Calmy A, et al. Ageing with HIV: medication use and risk for potential drug-drug interactions. J Antimicrob Chemother. 2011;66(9):2107–11.
9. Aouri M, Barcelo C, Ternon B, Cavassini M, Anagnostopoulos A, Yerly S, et al. In vivo profiling and distribution of known and novel phase I and phase II metabolites of efavirenz in plasma, urine, and cerebrospinal fluid. Drug Metab Dispos. 2016;44(1):151–61.
10. Ward BA, Gorski JC, Jones DR, Hall SD, Flockhart DA, Desta Z. The cytochrome P450 2B6 (CYP2B6) is the main catalyst of efavirenz primary and secondary metabolism: implication for HIV/AIDS therapy and utility of efavirenz as a substrate marker of CYP2B6 catalytic activity. J Pharmacol Exp Ther. 2003;306(1):287–300.
11. Robertson SM, Maldarelli F, Natarajan V, Formentini E, Alfaro RM, Penzak SR. Efavirenz induces CYP2B6-mediated hydroxylation of bupropion in healthy subjects. J Acquir Immune Defic Syndr. 2008;49(5):513–9.
12. Mouly S, Lown KS, Kornhauser D, Joseph JL, Fiske WD, Benedek IH, et al. Hepatic but not intestinal CYP3A displays dose-dependent induction by efavirenz in humans. Clin Pharmacol Ther. 2002;72(1):1–9.
13. Xu C, Desta Z. In vitro analysis and quantitative prediction of efavirenz inhibition of eight cytochrome P450 (CYP) enzymes: major effects on CYPs 2B6, 2C8, 2C9 and 2C19. Drug Metab Pharmacokinet. 2013;28(4):362–71.
14. German P, Greenhouse B, Coates C, Dorsey G, Rosenthal PJ, Charlebois E, et al. Hepatotoxicity due to a drug interaction between amodiaquine plus artesunate and efavirenz. Clin Infect Dis. 2007;44(6):889–91.
15. Wagner C, Pan Y, Hsu V, Grillo JA, Zhang L, Reynolds KS, et al. Predicting the effect of cytochrome P450 inhibitors on substrate drugs: analysis of physiologically based pharmacokinetic

modeling submissions to the US Food and Drug Administration. Clin Pharmacokinet. 2015;54(1):117–27.
16. Wagner C, Pan Y, Hsu V, Sinha V, Zhao P. Predicting the effect of CYP3A inducers on the pharmacokinetics of substrate drugs using physiologically based pharmacokinetic (PBPK) modeling: an analysis of PBPK submissions to the US FDA. Clin Pharmacokinet. 2016;55(4):475–83.
17. Moss DM, Marzolini C, Rajoli RKR, Siccardi M. Applications of physiologically based pharmacokinetic modeling for the optimization of anti-infective therapies. Expert Opin Drug Metab Toxicol. 2015;11(8):1203–17.
18. Siccardi M, Marzolini C, Seden K, Almond L, Kirov A, Khoo S, et al. Prediction of drug-drug interactions between various antidepressants and efavirenz or boosted protease inhibitors using a physiologically based pharmacokinetic modelling approach. Clin Pharmacokinet. 2013;52(7):583–92.
19. Siccardi M, Olagunju A, Seden K, Ebrahimjee F, Rannard S, Back D, et al. Use of a physiologically-based pharmacokinetic model to simulate artemether dose adjustment for overcoming the drug-drug interaction with efavirenz. In Silico Pharmacol. 2013;1:4.
20. Bosgra S, Eijkeren JV, Bos P, Zeilmaker M, Slob W. An improved model to predict physiologically based model parameters and their inter-individual variability from anthropometry. Crit Rev Toxicol. 2012;42(9):751–67.
21. Yu LX, Amidon GL. A compartmental absorption and transit model for estimating oral drug absorption. Int J Pharm. 1999;186(2):119–25.
22. Gertz M, Harrison A, Houston JB, Galetin A. Prediction of human intestinal first-pass metabolism of 25 CYP3A substrates from in vitro clearance and permeability data. Drug Metab Dispos. 2010;38(7):1147–58.
23. Rajoli RKR, Back DJ, Rannard S, Meyers F, Flexner C, Owen A, et al. Physiologically based pharmacokinetic modelling to inform development of intramuscular long-acting nanoformulations for HIV. Clin Pharmacokinet. 2015;54(6):636–50.
24. Oswald S, Meyer zu Schwabedissen HE, Nassif A, Modess C, Desta Z, Ogburn ET, et al. Impact of efavirenz on intestinal metabolism and transport: insights from an interaction study with ezetimibe in healthy volunteers. Clin Pharmacol Ther. 2012;91(3):506–13.
25. Barter ZE, Chowdry JE, Harlow JR, Snawder JE, Lipscomb JC, Rostami-Hodjegan A. Covariation of human microsomal protein per gram of liver with age: absence of influence of operator and sample storage may justify interlaboratory data pooling. Drug Metab Dispos. 2008;36(12):2405–9.
26. Poulin P, Theil FP. Prediction of pharmacokinetics prior to in vivo studies. 1. Mechanism-based prediction of volume of distribution. J Pharm Sci. 2002;91(1):129–56.
27. Jones HM, Parrott N, Jorga K, Lave T. A novel strategy for physiologically based predictions of human pharmacokinetics. Clin Pharmacokinet. 2006;45(5):511–42.
28. Säll C, Houston JB, Galetin A. A comprehensive assessment of repaglinide metabolic pathways: impact of choice of in vitro system and relative enzyme contribution to in vitro clearance. Drug Metab Dispos. 2012;40(7):1279–89.
29. Filppula AM, Laitila J, Neuvonen PJ, Backman JT. Reevaluation of the microsomal metabolism of montelukast: major contribution by CYP2C8 at clinically relevant concentrations. Drug Metab Dispos. 2011;39(5):904–11.
30. Jaakkola T, Laitila J, Neuvonen PJ, Backman JT. Pioglitazone is metabolised by CYP2C8 and CYP3A4 in vitro: potential for interactions with CYP2C8 inhibitors. Basic Clin Pharmacol Toxicol. 2006;99(1):44–51.
31. Hanioka N, Matsumoto K, Saito Y, Narimatsu S. Functional characterization of CYP2C8.13 and CYP2C8.14: catalytic activities toward paclitaxel. Basic Clin Pharmacol Toxicol. 2010;107(1):565–9.
32. Abel S, Jenkins TM, Whitlock LA, Ridgway CE, Muirhead GJ. Effects of CYP3A4 inducers with and without CYP3A4 inhibitors on the pharmacokinetics of maraviroc in healthy volunteers. Br J Clin Pharmacol. 2008;65(1):38–46.
33. Varma MVS, Lai Y, Kimoto E, Goosen TC, El-Kattan AF, Kumar V. Mechanistic modeling to predict the transporter- and enzyme-mediated drug-drug interactions of repaglinide. Pharm Res. 2013;30(4):1188–99.
34. Siccardi M, D'Avolio A, Nozza S, Simiele M, Baietto L, Stefani FR, et al. Maraviroc is a substrate for OATP1B1 in vitro and maraviroc plasma concentrations are influenced by SLCO1B1 521 T>C polymorphism. Pharmacogenet Genomics. 2010;20(12):759–65.
35. Nieuweboer AJ, Hu S, Gui C, Hagenbuch B, Ghobadi Moghaddam-Helmantel IM, Gibson AA, et al. Influence of drug formulation on OATP1B-mediated transport of paclitaxel. Cancer Res. 2014;74(11):3137–43.
36. Vrouenraets SM, Wit FW, van Tongeren J, Lange JM. Efavirenz: a review. Expert Opin Pharmacother. 2007;8(6):851–71.
37. Hatorp V, Huang WC, Strange P. Repaglinide pharmacokinetics in healthy young adult and elderly subjects. Clin Ther. 1999;21(4):702–10.
38. Hegazy SK, Mabrouk MM, Elsisi AE, Mansour NO. Effect of clarithromycin and fluconazole on the pharmacokinetics of montelukast in human volunteers. Eur J Clin Pharmacol. 2012;68(9):1275–80.
39. Tornio A, Niemi M, Neuvonen PJ, Backman JT. CYP2C8*3 allele have opposite effects on the pharmacokinetics of pioglitazone. Drug Metab Dispos. 2008;36(1):73–80.
40. Villalona-Calero MA, Weiss GR, Burris HA, Kraynak M, Rodrigues G, Drengler RL, et al. Phase I and pharmacokinetic study of the oral fluoropyrimidine capecitabine in combination with paclitaxel in patients with advanced solid malignancies. J Clin Oncol. 1999;17(6):1915–25.
41. Abduljalil K, Cain T, Humphries H, Rostami-Hodjegan A. Deciding on success criteria for predictability of pharmacokinetic parameters from in vitro studies: an analysis based on in vivo observations. Drug Metab Dispos. 2014;42(9):1478–84.
42. Naraharisetti SB, Lin YS, Rieder MJ, Marciante KD, Psaty BM, Thummel KE, et al. Human liver expression of CYP2C8: gender, age, and genotype effects. Drug Metab Dispos. 2010;38(6):889–93.
43. Kajosaari LI, Laitila J, Neuvonen PJ, Backman JT. Metabolism of repaglinide by CYP2C8 and CYP3A4 in vitro: effect of fibrates and rifampicin. Basic Clin Pharmacol Toxicol. 2005;97(4):249–56.
44. Maekawa K, Harakawa N, Yoshimura T, Kim SR, Fujimura Y, Aohara F, et al. CYP3A4*16 and CYP3A4*18 alleles found in East Asians exhibit differential catalytic activities for seven CYP3A4 substrate drugs. Drug Metab Dispos. 2010;38(12):2100–4.
45. Bidstrup TB, Stilling N, Damkier P, Scharling B, Thomsen MS, Brosen K. Rifampicin seems to act as both an inducer and an inhibitor of the metabolism of repaglinide. Eur J Clin Pharmacol. 2004;60(2):109–14.
46. Jamis-Dow CA, Pearl ML, Watkins PB, Blake DS, Klecher RW, Collins JM. Predicting drug interactions in vivo from experiments in vitro. Human studies with paclitaxel and ketoconazole. Am J Clin Oncol. 1997;20(6):592–9.
47. Honkalammi J, Niemi M, Neuvonen PJ, Backman JT. Gemfibrozil is a strong inactivator of CYP2C8 in very small multiple doses. Clin Pharmacol Ther. 2012;91(5):846–55.
48. Karonen T, Neuvonen PJ, Backman JT. CYP2C8 but not CYP3A4 is important in the pharmacokinetics of montelukast. Br J Clin Pharmacol. 2012;73(2):257–67.

49. Brännström M, Nordell P, Bonn B, Davis AM, Palmgren AP, Hilgendorf C, et al. Montelukast disposition: no indication of transporter-mediated uptake in OATP2B1 and OATP1B1 expressing HEK293 cells. Pharmaceutics. 2015;7(4):554–64.
50. Jaakkola T, Backman JT, Neuvonen M, Laitila J, Neuvonen PJ. Effect of rifampicin on the pharmacokinetics of pioglitazone. Br J Clin Pharmacol. 2006;61(1):70–8.
51. Backman JT, Filppula AM, Niemi M, Neuvonen PJ. Role of cytochrome P450 2C8 in drug metabolism and interactions. Pharmacol Rev. 2016;68(1):168–241.
52. DrugBank. http://www.drugbank.ca. Accessed 1 Apr 2016.
53. Chemicalize.org. http://www.chemicalize.org. Accessed 1 Apr 2016.
54. Hyland R, Dickins M, Collins C, Jones H, Jones B. Maraviroc: in vitro assessment of drug-drug interaction potential. Br J Clin Pharmacol. 2008;66(4):498–507.
55. Brouwer E, Verweij J, De Bruijn P, Loos WJ, Pillay M, Buijs D, et al. Measurement of fraction unbound paclitaxel in human plasma. Drug Metab Dispos. 2000;28(10):1141–5.
56. Croteau D, Best BM, Letendre S, Rossi SS, Ellis RJ, Clifford DB, et al. Lower than expected maraviroc concentrations in cerebrospinal fluid exceed the wild-type CC chemokine receptor 5-tropic HIV-1 50 % inhibitory concentration. AIDS. 2012;26(7):890–3.
57. Mougey EB, Feng H, Castro M, Irvin CG, Lima JJ. Absorption of montelukast is transporter mediated: a common variant of OATP2B1 is associated with reduced plasma concentrations and poor response. Pharmacogenet Genomics. 2009;19(2):129–38.
58. Alani AW, Rao DA, Seidel R, Wang J, Jiao J, Kwon GS. The effect of novel surfactants and Solutol HS 15 on paclitaxel aqueous solubility and permeability across a Caco-2 monolayer. J Pharm Sci. 2010;99(8):3473–85.
59. Nordisk Novo. Prandin summary of product characteristics. Gatwick: Novo Nordisk; 2012.
60. Bristol-Myers-Squibb. Sustiva summary of product characteristics. Uxbridge: Bristol-Myers-Squibb; 2011.
61. Takeda. Actos summary of product characteristics. Taastrup: Takeda; 2013.
62. Merck Sharp & Dohme. Singulair summary of product characteristics. Hoddesdon: Merck Sharp & Dohme; 2015.
63. Bristol-Myers-Squibb. Taxol summary of product characteristics. Uxbridge: Bristol-Myers-Squibb; 2011.
64. ViiV. Selzentry summary of product characteristics. Brentford: ViiV; 2015.
65. Csajka C, Marzolini C, Fattinger K, Decosterd LA, Fellay J, Telenti A, et al. Population pharmacokinetics and effects of efavirenz in patients with human immunodeficiency virus infection. Clin Pharmacol Ther. 2003;73(1):20–30.
66. Cheng H, Leff JA, Amin R, Gertz BJ, De Smet M, Noonan N, et al. Pharmacokinetics, bioavailability, and safety of montelukast sodium (MK-0476) in healthy males and females. Pharm Res. 1996;13(3):445–8.
67. Mross K, Holländer N, Hauns B, Schumacher N, Maier-Lenz H. The pharmacokinetics of a 1-h paclitaxel infusion. Cancer Chemother Pharmacol. 2000;45(6):463–70.